ISSN: 0067-2904

The Effect of Au Nanoparticles on the Structural and Optical Properties of (NiO:WO3) Thin Films Prepared by PLD Technique

Ali sh. Maktoof*, GhusonH.Mohammed
Physics Dep., College of Science, University of Baghdad, Baghdad, Iraq

Received: 25/4/2021 Accepted: 22/8/2021 Published: 30/6/2022

Abstract

In the present investigation, ($NiO:WO_3$) thin films were deposited at RT onto glass substrates using PLD technique employing focused Nd:YAG laser beam at 600 mJ with a frequency second radiation at 1064 nm (pulse width 9 ns) repetition frequency (6 Hz), for 400 laser pulses incident on the target surface .The structural, morphological and optical properties of the films doped with different concentration of Au content (0.03, 0.05, and 0.07) were examined with X-ray diffractometer(XRD), Atomic Force Microscope(AFM) , UV–Vis spectrophotometer . The results show that the films were amorphous with small peaks appearing when doped with AuNPs . The XRD peaks of the deposited NiO:WO3 were enhanced with increasing the Au content . The crystalline size of the deposited thin films was calculated using Debye Scherer formula and found to decrease from 6.6 nm for undoped NiO:WO3 to 3.4 nm for doped (NiO:WO3) with the increase of Au content from x=0 to x=0.07 at preferred orientation of (200). All the samples have a cubic structure. Also, the results showed that Au content of the films affects the surface morphology. From the results of AFM analysis, it was found that the roughness and average diameter change when adding Au to the structure, with the highest value occurring at Au ratio 0.03 equal to 7.58 and 81.02 nm, respectively. UV–Vis spectrophotometer was used to investigate the optical transmission. It was found that when Au content of films increased, the transmittance of films decreased.

Keywords: Structural properties, optical properties, NiO :WO3 thin films, Au nanoparticles

تأثير جسيمات الذهب النانوية على الخواص الهيكلية والبصرية للأغشية الرقيقة (اوكسيد النيكل و اوكسيد التنكستن) المحضرة باستخدام تقنية الترسيب بالليزر النبضي

علي شريف مكطوف*, غصون حميد محمد
قسم الفيزياء, كلية العلوم, جامعة بغداد، بغداد، العراق

الخلاصة

في هذا التحقيق ، تم تحضير أغشية رقيقة (NiO: WO3) في درجة حرارة الغرفة على ركائز زجاجية باستخدام تقنية PLD مع شعاع ليزر Nd: YAG المركّز عند 600 مللي جول مع تردد إشعاع عند 1064 نانومتر (عرض النبضة 9 نانوثانية) تردد تكرار (6) Hz) لـ 400 نبضة ليزر وقعت على السطح المستهدف.

*Email: alishmk4@gmail.com

تم فحص الخصائص التركيبية والمورفولوجية والبصرية للأغشية بواسطة حيود الأشعة السينية (XRD) ، مجهر القوة الذرية (AFM) ، التحليل الطيفي للأشعة فوق البنفسجية– المرئية ، على التوالي بتركيزات مختلفة محتوى الذهب (0.03, 0.05 و 0.07).أظهرت النتائج أن الأفلام كانت غير متبلورة مع ظهور قمم صغيرة عند التطعيم بمادة الذهب.تم تحسين قمم XRD الخاصة بـNiO:WO3 المرسبة مع زيادة محتوى الذهب. تم حساب الحجم البلوري للأغشية الرقيقة المرسبة باستخدام علاقة Debye Scherer ووجد انخفاض من 6.6 نانومتر لـ NiO:WO3 إلى 3.4 نانومتر لاغشية (NiO:WO3) مع زيادة محتوى الذهب من x=0 الى x=0.07 في الاتجاه المفضل لـ (200) وتبين ان جميع العينات لها هيكل مكعب . أظهرت النتائج أيضًا أن محتوى الذهب للأغشية يؤثر على شكل السطح. من نتائج تحليل AFM ، وجد أن الخشونة ومعدل الحجم الحبيبي تتغير عند إضافة الذهب إلى الهيكل ، مع أعلى قيمة تحدث عند نسبة 0.03من الذهب يساوي إلى 7.58 و81.02 nm. تم استخدام المطياف البصري UV–Vis لاستقصاء طيف النفاذ. لقد وجد أنه عندما زاد محتوى الذهب في الاغشية المحضرة ، تقل نفاذية الاغشية المحضرة.

1.Introduction

Research on transition elements has led to the conclusion that different classes of materials are of particular interest for various applications such as in nanoscale, microelectronics, computer science, energy, transportation, safety engineering, military, technology, optoelectronic devices and electrical appliances, etc.[1]. Nickel oxide (NiO) and tungsten oxide (WO_3) are regarded as two of the best frequently used transition oxides, which provide a set of new and diverse properties, especially in the form of thin films [2]. It is known that the mixed nickel–tungsten oxides have much better properties than their pure counterparts, especially tungsten [3, 4], As well as nickel [5]. Nickel oxide is a material that has many uses and applications due to its special features, such as p-type transparent conductive film, electrical devices, gas sensors, magnetic storage materials, active optical electrodes, dye sensitivity, solar cells etc. [6,7]. In recent years, interest has increased in tungsten oxide (WO_3) due to its importance in photocatalysis and photovoltaics[8]. Also, it is an n-type semiconductor with a bandgap of 2.5–3.0 eV; it can be employed as a sensing layer [9]. This material has many characteristics that make it distinctive, including its cheapness, chemical stability, non-toxicity and mechanical properties; Also, it is considered a catalyst for semiconductors [10,11]. On the other hand, the metallic noble Au nanoparticles are attracting much attention because of their excellent electrical efficiency, optical, physical, chemical and magnetic properties[12,13]. Also, it has pulsed photoabsorption, high dispersion in an aqueous medium, chemical inertness, and biocompatibility [14,15].

In the present paper, the fabrication and characterization of optically transparent (NiO:WO3) films and doped with different content of Au nanoparticles were investigated. The structural, morphological and optical properties of the (NiO:WO3):Au thin films were characterized by X-ray diffraction (XRD), atomic force microscopy (AFM) and UV–Visible spectroscopy.

2.Experimental

(2-1) Preparation of Samples

$NiO_{0.85}$:$WO_{0.15}$ with (99.99% purity) was mixed with different contents of Au nanoparticles (0.03,0.05, 0.07). The powder was gridded together for 10 minutes using a gate mortar. After that, it was compressed together with a hydraulic press under 5 tons pressure for (10 minutes) to have pellets of 1 cm diameter and 0.2 cm thickness. The pellets were sintered at (700 ° C) for one hour; after that, they were cooled to room temperature.

(2-2) Deposition of Thin Films

The prepared pellets were used to deposit $(NiO:WO_3)_{1-x}Au_x$ thin films at room temperature(RT) on glass substrates with dimensions (2,5×7,5 cm) which were washed with distilled water using an ultrasonic procedure for 15 minutes. Thin films were prepared using the pulsed laser deposition technique employing Nd: YAG laser with a wavelength of (1064 nm) and energy 600 mJ, for 400 laser pulses, replicate frequency (6Hz) incident on the target

surface with a 45 ° angle. The deposition was made at a chamber pressure of (1×10^{-1}) mbar. The target-substrate distance was 10cm. The film thickness was estimated using the interference method to be around 200±5 nm.

(2-3)Measurements

The structural property of $(NiO:WO3)_{1-x}Au_x$ thin films was examined by X-ray diffractometer (Philips PW1730) using Cu-Kα (λ = 0.154 nm) over a 2θ scan range of 10–80°. The surface morphological property of the film was studied by atomic force spectroscopy (AFM). The optical properties of thin films were studied using UV–Vis-NIR spectrophotometer (Metertech, SP8001) in the wavelength range of (190-1100) nm

3. results and the discussions

(3-1) The X-rays Diffraction Results .

Figure 1 shows the x-ray diffraction patterns (XRD) of undoped and doped NiO:WO3 thin films with different Au content. The results showed that the films were amorphous. This result agrees with Myong et al. [12] and with Ayat et al. [13]. The XRD pattern showed very weak peaks at an angle of 43.3721 corresponding to a reflection of (200). This may be due to the addition of tungsten into NiO inducing a weakening of the long-range order in the Ni-O matrix. [16]. It was noted that when Au of (0.05 and 0.07) content was added to the films, two new weak peaks appeared at an angle of 37.186 corresponding to a reflection of (111). This is an indication of the effect of gold content. It was found that, (NiO: WO3): Au thin films have cubic structure, compared with those given in the (ASTM data card No.96-432-0488).

To calculate the size of the crystal (C_s), the Debye-Scherer equation was used [17]:

$$C_s = \frac{0.9\,\lambda}{\beta \cos\theta} \quad (1)$$

Where: λ is the wavelength of the X-ray, $\boldsymbol{\beta}$is the full width at half maximum (FWHM) and θ is the diffraction angle.

to calculate the strain(ε), the following relation was used[18]:

$$\varepsilon = \frac{\beta_{hkl}}{4\,tan\theta} \quad (2)$$

To find the dislocation density (δ) that can be represented by the length of the dislocation lines to the crystal size, the following relation was applied [19]:

$$\delta = \frac{1}{C_s^2} \quad (3)$$

The average crystallite size Cs, inter-planner distance, microstrain ε dislocation and number of planes were also calculated according to Debye Scherer equation. The results are presented in Table 1 for (100) and (200) planes in the diffraction pattern of undoped and doped $NiO:WO_3$ thin films.

According to data from Table 1, it was noted that the average crystallite size had decreased, and the micro-strain and dislocation increased with the increase of the Au content. This should be ascribed to Au phase inhibiting the (NiO:WO3) grain growth. It can also be attributed to the fact that the atomic radii of Au particles are less than that of NiO leading to Myong et al. [12] and with Ayat et al. [13]. The XRD pattern showed very weak peaks at an angle of 43.3721 corresponding to a reflection of (200). This may be due to the addition of tungsten into NiO inducing a weakening of the long-range order in the Ni-O matrix. [16]. It was noted that when Au of (0.05 and 0.07) content was added to the films, two new weak peaks appeared at an angle of 37.186 corresponding to a reflection of (111).

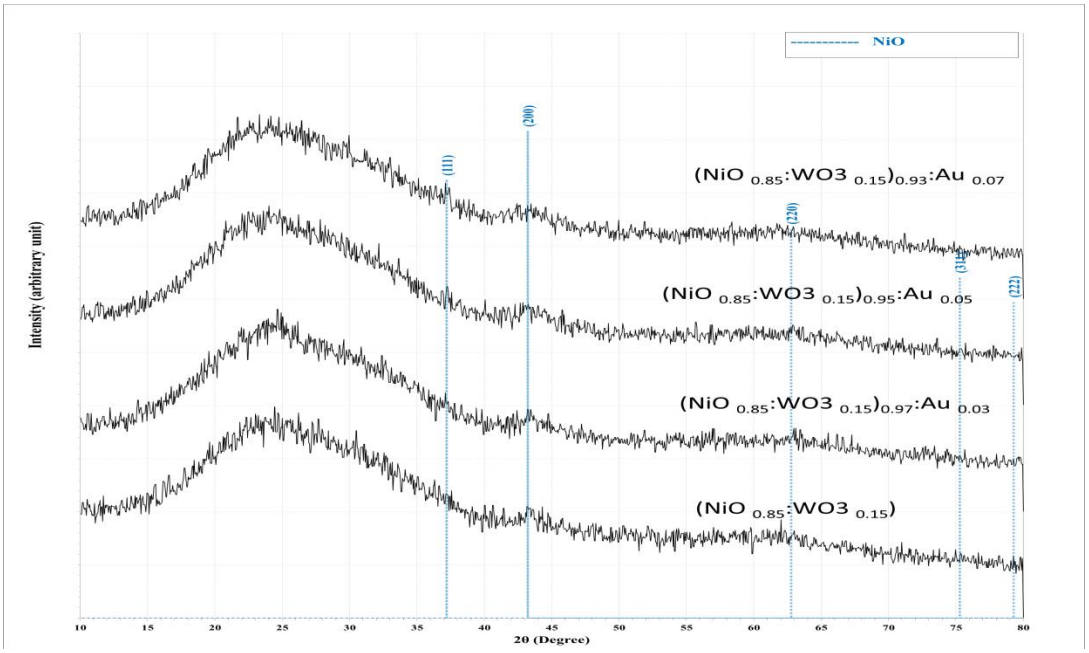

Figure 1- the X-ray diffraction of (NiO $_{0.85}$:WO3 $_{0.15}$) doped with different contents of Au nanoparticles.

Table 1- the interplaner distance (d_{hkl},), FWHM (deg.), and crystal size for (NiO:WO3) thin filmsdoped with different contents of Au nanoparticles.

Au (%)	2θ (Deg.)	FWHM (Deg.)	d_{hkl} Exp.(Å)	C.S (nm)	d_{hkl} Std.(Å)	$\varepsilon\times10^{-3}$	$\delta(nm)^{-2}$	hkl	Phase
(NiO $_{0.85}$:WO3 $_{0.15}$)	43.3721	1.3023	2.0846	6.6	2.0824	818.7140	23.2034	(200)	Cubic NiO
(NiO $_{0.85}$:WO3 $_{0.15}$)$_{0.97}$):Au $_{0.03}$(	43.3721	1.4651	2.0846	5.8	2.0824	921.0611	29.3673	(200)	Cubic NiO
((NiO $_{0.85}$:WO3 $_{0.15}$) $_{0.95}$):Au $_{0.05}$	37.1860	0.9225	2.4159	9.1	2.4044	685.5654	12.1133	(111)	Cubic NiO
	43.3721	2.1163	2.0846	4.0	2.0824	1330.4496	61.2751	(200)	Cubic NiO
((NiO $_{0.85}$:WO3 $_{0.15}$)$_{0.93}$):Au $_{0.07}$	43.2636	2.5503	2.0896	3.4	2.0824	1607.7230	89.0510	(200)	Cubic NiO

(3-2) Atomic force microscopic

3D AFM images of (NiO:WO3) thin films doped with different content of Au nanoparticles are shown in Figure 2 and Table 2 from which the surface morphology of films deposited on glass substrates at 300 K can be studied, and the mean diameter, mean roughness, and mean square root (RMS) can be determined. The fine morphology and roughness of the films of (NiO:WO3) with different activators of Au can be observed. The images show a well aligned printed AuNPs monolayer covered by (NiO:WO3). The mean size of Au-doped NiO:WO3,determined from the images, was larger than that calculated from XRD data, which can be attributed to the particle conglomeration. The brighter contrast in the image indicates the heavier element (Au in our case).

Adding Au resulted in roughness and RMS change, with the highest value occurring at Au ratio of 0.03. According to the XRD and AFM results, the 0.03 Au ratio is the best among the

other ratios (It gave the largest crystalline size and the highest roughness), and it can be used to make various devices such as optoelectronic devices.

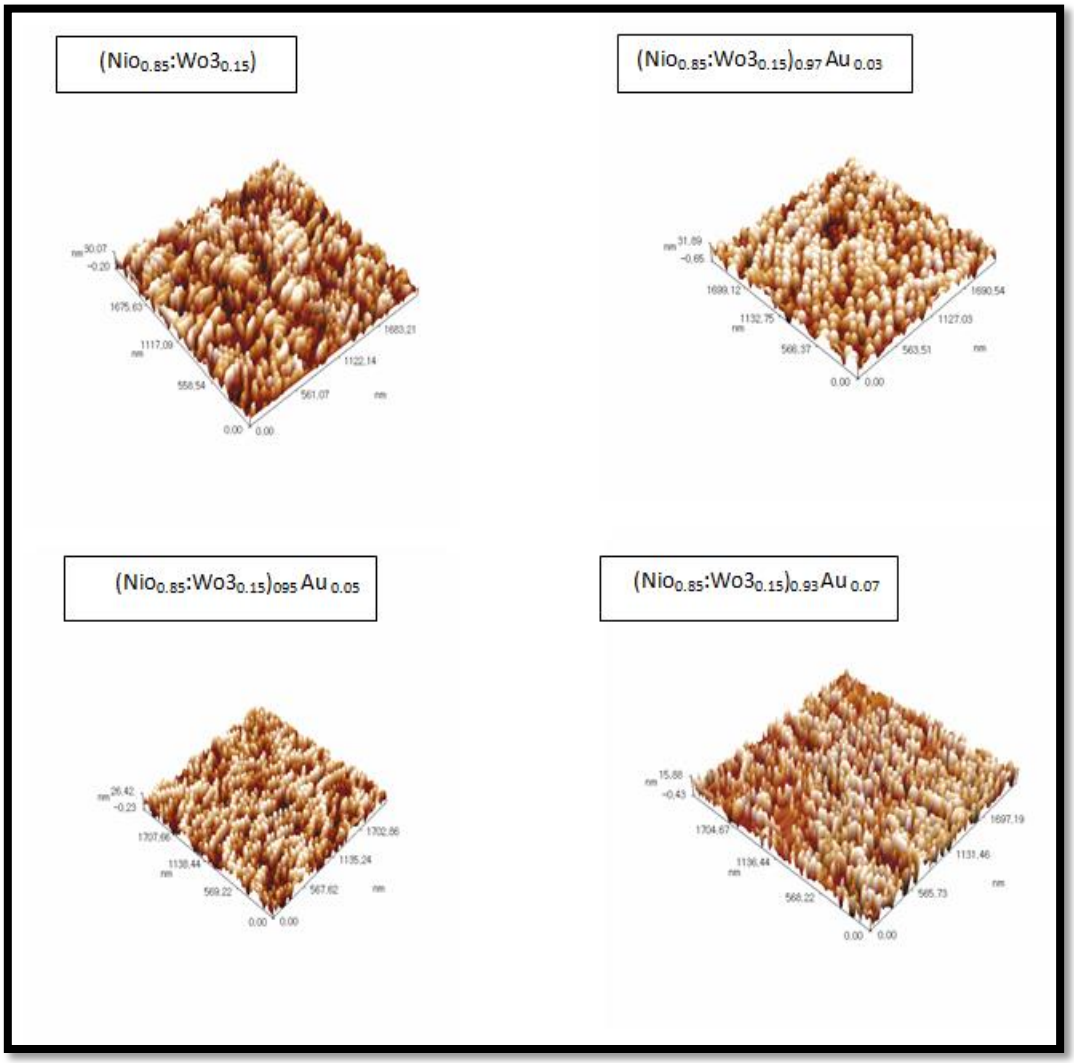

Figure 2- 3D AFM images of $(NiO)_{0.85}:(WO_3)_{0.15}$ thin films doped with different contents of Au nanoparticles prepared at room temperature.

Table 2: overall roughness of the surface and granular content of the prepared films at room temperature

Sample	Avg.Diameter (nm)	Avg.Roughness (nm)	R.M.S (nm)	Peak-peak (nm)
$(NiO)_{0.85}:(WO_3)_{0.15}$	59.96	7.57	8.74	30.3
$((NiO)_{0.85}:(WO_3)_{0.15})_{0.97}:Au_{0.03}$	81.02	7.58	8.9	32.5
$((NiO)_{0.85}:(WO_3)_{0.15})_{0.95}:Au_{0.05}$	60.92	6.86	7.87	26.6
$((NiO)_{0.85}:(WO_3)_{0.15})_{0.93}:Au_{0.07}$	56.22	4.1	4.73	16.3

(3-3)The optical properties

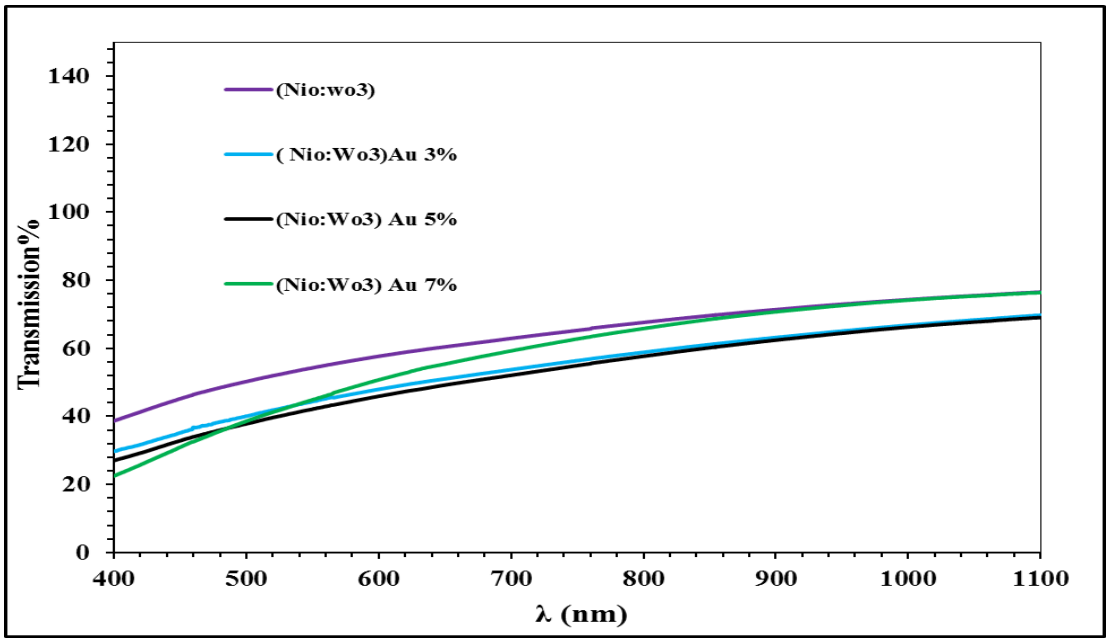

Figure 3-Transmittance spectra of (NiO) 0.85:(WO3)0.15 thin films doped with different contents of Au nanoparticles.

The optical properties of undoped and doped (NiO:WO_3) thin films with different content of Au (0.03, 0.05 and 0.07)%wt., such as transmission, absorption coefficient, extinction coefficient, refractive index, dielectric constant, and optical energy gap were measured and recorded in the wavelength range of (400-1100) nm. Figure 3 shows the transmission change with wavelength for (NiO:WO3):Au prepared at RT. It is evident from the figure and Table 3 that the transmittance value is inversely proportional to the Au concentration; it decreased with the increase of the Au content in (NiO:WO3) films. This may be due to the increase of heavy atoms which cause the increase in absorption. On the other hand, the decrease of the transmission may be attributed to the creation of levels at the energy bandgap leading to the shift of peak to smaller energies. This result agrees with that of Khorsand [20]. This result may also be explained because adding Au particles to the NiO :WO_3 matrix adds excess oxygen(a decrease in Ni^{2+} ions and an increase in Ni^{3+} ions), thus producing nickel vacancies. According to Mendoza-Galvan et al., excess oxygen in the lattice causes absorption of wavelengths longer than 400 nm [18]. It was also noticed, from the figure, that the transmission of undoped (NiO:WO3) is higher than that of the Au doped (NiO:WO3)[21]. This result agrees with the XRD and AFM analysis.

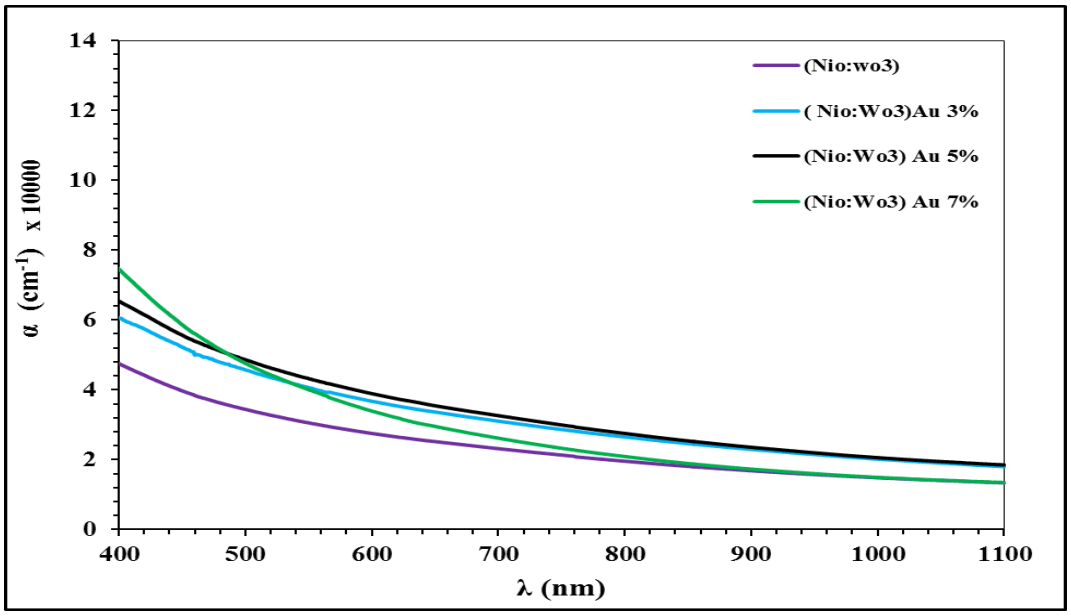

Figure 4-Absorption coefficient of $(NiO)_{0.85}:(WO_3)_{0.15}$ thin films doped with different contents of Au nanoparticles.

The absorption coefficient can be found through the relation[22,23]:

$$\alpha = 2.303A/t \quad (4)$$

where: A is the absorbance and t is the thickness of the sample.

The value of the optical energy gap can be calculated through the following relation[24]:

$$\alpha h\nu = B(h\nu - Eg)^r \quad (5)$$

where Eg is the optical bandgap, r is the exponent indicating the type of optical transitions in the material, hν is the energy of the incident photon, B is a constant inversely proportion with the degree of amorphousity. experiences a strong increase in absorption due to band-to-band absorption, which occurs when an electron is elevated from the valence band to the conduction band, resulting in the formation of a new pair of charge carriers (an electron and a hole). The high absorption and low transmittance in the UV region of the doped $NiO:WO_3$ thin films (as seen in Figure 5) may be helpful in blocking the UV portion of the electromagnetic spectrum, which is harmful to human health. Additionally, as the doping value increases, the energy gap values decrease. Table 3 shows the bandgap values for the different Au content. The decrease of Eg with the increase of Au content (x) increases the absorbance making the material opaque. This is due to the increase of the density of localized states in the Eg near valence band or conduction band, which are ready to receive electrons and generate tails in the optical energy gap reducing the energy gap. The decrease in the bandgap can also be correlated to many-body interaction effects, which occurs between either free carriers and ionized impurities or charge carriers [25]. From Figure 5, it can be observed that increasing Au content from 0 to 7% leads to decrease in the optical bandgap values from approximately 3.25 eV to 2.7 eV at RT. This result agrees with that of and is compatible with the XRD results.

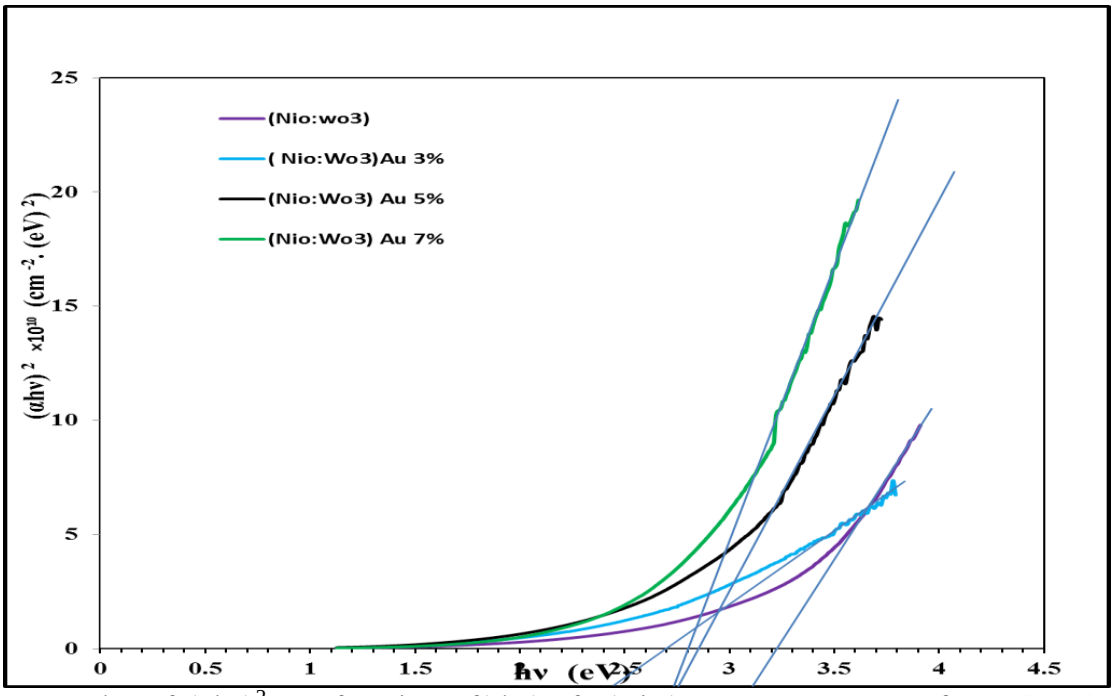

Figure 5-Plot of $(\alpha h\upsilon)^2$ as afunction of(hυ) for$(NiO)_{0.85}:(WO_3)_{0.15}$ thin films doped with different contents of Au nanoparticles.

The variation of extinction coefficient (k) with wavelength in the range of (400 - 1100) nm for samples prepared at room temperature is shown in Figure 6, which shows that the k values increase with the increase of the doping. The results are illustrated in Table 3. The values of k were determined from the following relation[26]

$$k=\frac{\alpha\lambda}{4\pi} \quad (6)$$

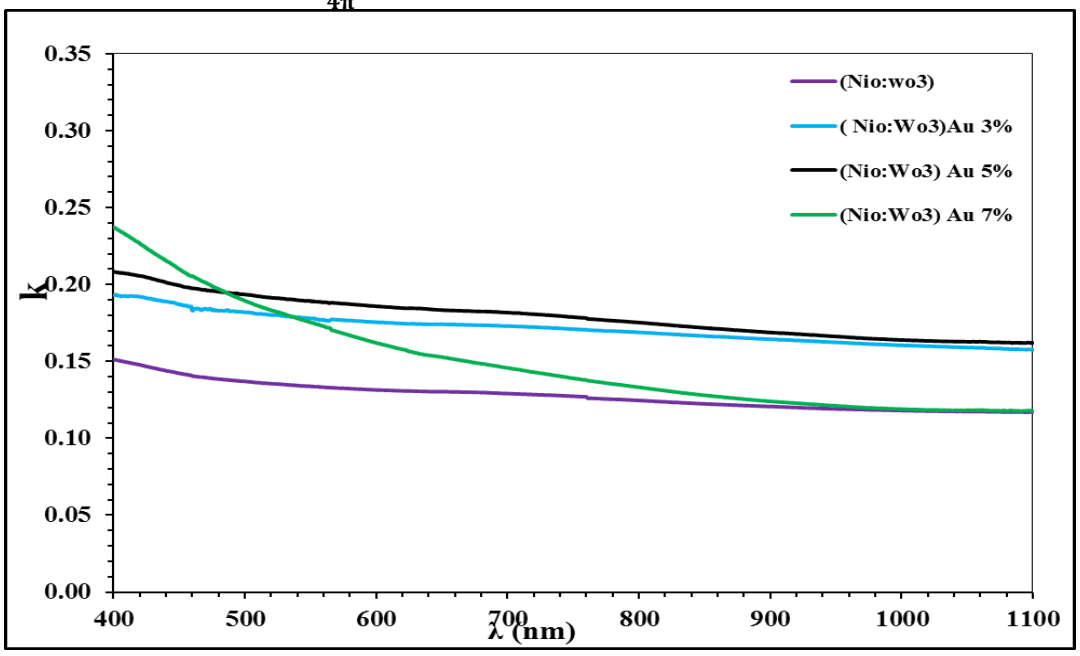

Figure 6-The extinction coefficient (k) for $(NiO)_{0.85}:(WO_3)_{0.15}$ thin films doped with different content of Au nanoparticles.

The variation of refractive index with wavelength of undoped and doped ($NiO:WO_3$) with different (Au) content in the wavelength range of (400-1100)nm is shown in Figure 7 and Table 3, as can be noted that the refractive index decreases as the doping increases.

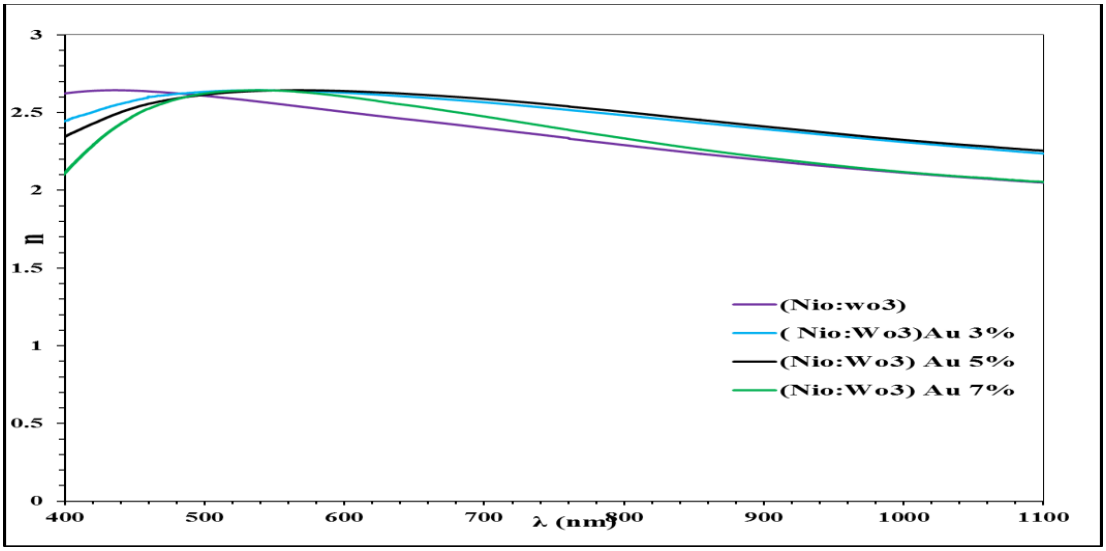

Figure 7-Refractive index for $(NiO)_{0.85}:(WO_3)_{0.15}$ thin films doped with different contents of Au nanoparticles.

Relation 7 describes the complex optical refractive index of thin films[27]:

$$n^*=n - ik \quad (7)$$

Where: n* is the complex refractive index, (n) and (k) are the real part and imaginary part of a complex refractive index. While, the simple refractive index can be found through the relation[28]:

$$n=\frac{1+R}{1-R}+\sqrt{\frac{4R}{(1-R)2}}-K2 \quad (8)$$

Figures.8 and 9 show the real and imaginary part of the dielectric constant of undoped and doped ($NiO:WO_3$) thin films with different contents of Au (0.03,0.05,0.07), respectively, as a function of wavelength in the wavelength range (400-1100) nm at room temperature. The real part (according to Equation 9) depends only on the value of (n^2) since (k^2) is very small compared to n^2. While, the imaginary part (according to Equation 10) depends on the value of (k). It was found that their values increased with increasing the doping , and with increasing wavelength, and as shown in Table 3. The real and imaginary parts of the dielectric constant were calculated by applying the equations [29]:

$$\varepsilon_r = n^2-k^2 \quad (9)$$

$$\varepsilon_i = 2nk \quad (10)$$

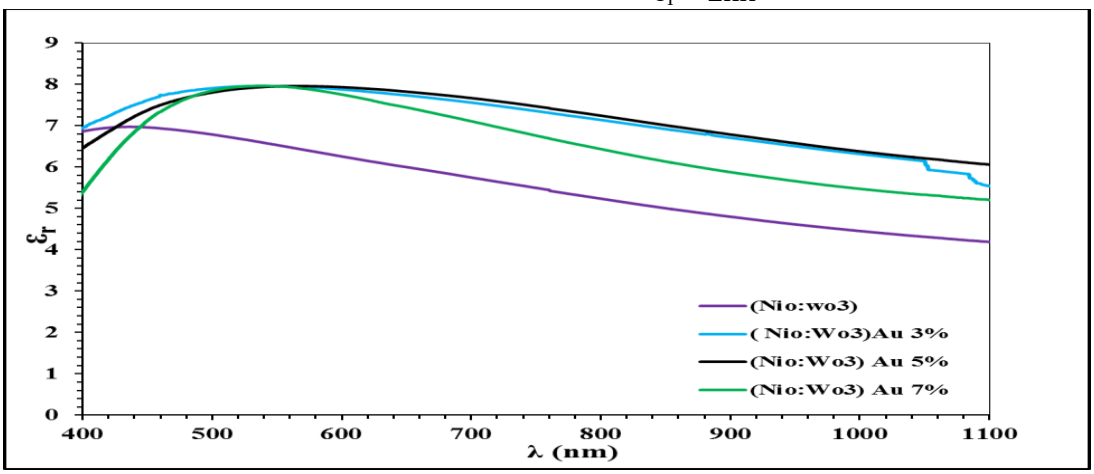

Figure 8-The real part of the dielectric constant for $(NiO)_{0.85}:(WO_3)_{0.15}$ thin films doped with different contents of Au nanoparticles.

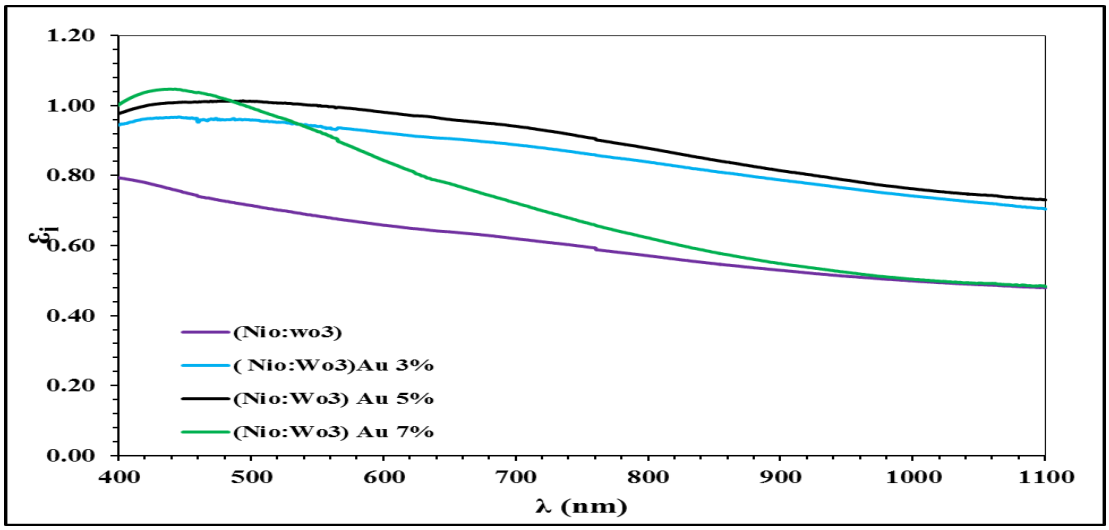

Figure 9-The imaginary part of the dielectric constant for $(NiO)_{0.85}:(WO_3)_{0.15}$ thin films doped with different contents of Au nanoparticles.

Table 3-The transmittance, absorption coefficient and optical constant for $((NiO)_{0.85}:(WO_3)_{0.15})$ thin films undoped and doped with (Au) in proportions (0.03,0.05,0.07) at room temperature.

Sample	T%	α (cm^{-1})	k	n	ε_r	ε_i	Eg (eV)
$(NiO)_{0.85}:(WO_3)_{0.15}$	50.24	34417	0.137	2.623	6.786	0.715	3.25
$((NiO)_{0.85}:(WO_3)_{0.15})_{0.97}:Au_{0.03}$	40.11	45682	0.182	2.446	7.907	0.958	2.70
$((NiO)_{0.85}:(WO_3)_{0.15})_{0.97}:Au_{0.05}$	37.82	48613	0.194	2.345	7.801	1.012	2.85
$((NiO)_{0.85}:(WO_3)_{0.15})_{0.97}:Au_{0.07}$	38.62	47567	0.189	2.111	7.845	0.993	2.80

Conclusion

In the present work, the effect of doping **(NiO: WO3) thin films** with different Au content on the structural, morphological and optical properties was studied. The XRD pattern showed that the films are amorphous with the presence of very small weak peaks at an angle of 43.3721 corresponding to a reflection of 200 which is developed after annealing temperature. According to the XRD and AFM analysi, the ratio of 0.03 percent Au is the best among the other ratios (It gave the highest crystalline size and the highest roughness); it can be used to make a variety of products, including optoelectronic devices. For all samples, the absorption coefficient decreased as the doping ratio increased, and had a value of (> 104 cm^{-1}). It was found that the refractive index decreased, extinction coefficient increased and dielectric constant (real and imaginary parts) increased with the increase of the ratio of doping. From the results, it was concluded that NiO: WO_3 doped with different content of Au is a perfect device in solar cell applications.

References

[1] K. Gesheva, M. Arvizu, G. Bodurov, T. Ivanova, G. Niklasson, I. M. Szilagyi, "Optical, structural and electrochromic properties of sputter- deposited W-Mo oxide thin films," *J. Phys. Conf. Ser.*, vol. 764, pp. 1-10, 2016, doi: 10.1088/1742-6596/764/1/012010.

[2] K. S. Usha, R. Sivakumar, C. Sanjeeviraja, and M. Ichimura, "Physical properties of rf magnetron sputter deposited NiO:WO3 thin films," *Mater. Res. Express*, vol. 2, no. 1, p. 16401, 2015, doi: 10.1088/2053-1591/2/1/016401.

[3] Shen P K, Syed-Bokhari J and Tseung A C C 1991 *J. Electrochem. Soc*. 138 2778

[4] Green S V, Pehlivan E, Granqvist C G and Niklasson G A 2012 Sol. *Energy Mater. Sol. Cells* 99 339

[5] Lee S H and Joo S K 1995 Sol. *Energy Mater. Sol. Cells* 39 155

[6] S. Kim, M. Taya, and C. Xu, "Contrast, Switching Speed, and Durability of V[sub 2]O[sub 5]–TiO[sub 2] Film-Based Electrochromic Windows," *J. Electrochem. Soc*., vol. 156, no. 2, pp. E40-E45, 2009, doi: 10.1149/1.3031978.

[7] T. Dutta, P. Gupta, A. Gupta, and J. Narayan, "Effect of Li doping in NiO thin films on its transparent and conducting properties and its application in heteroepitaxial p-n junctions," *J. Appl. Phys*., vol. 108, no. 8, pp. 0–7, 2010, doi: 10.1063/1.3499276.

[8] F. Mitsugi, E. Hiraiwa, T. Ikegami, K. Ebihara, and R. K. Thareja, "WO3 thin films prepared by pulsed laser deposition," *Japanese J. Appl. Physics*, vol. 41, no. 8, pp. 5372–5375, 2002, doi: 10.1143/jjap.41.5372.

[9] I. Castro-Hurtadoa,∗, T. Taveraa, P. Yurritaa, N. Pérez a, A. Rodriguez b, G.G. Mandayoa, E. Castano,"Structural and optical properties of WO3 sputtered thin films nanostructured by laser interference lithography," *Applied Surface Science*, vol. 276, pp.229-235. 2013.

[10] S. K. Gullapalli, R. S. Vemuri, and C. V. Ramana, "Structural transformation induced changes in the optical properties of nanocrystalline tungsten oxide thin films," *Appl. Phys. Lett*., vol. 96, no. 17, pp. 20–23, 2010, doi: 10.1063/t1.3421540.

[11] K. J. Patel, C. J. Panchal, V. A. Kheraj, and M. S. Desai, "Growth, structural, electrical and optical properties of the thermally evaporated tungsten trioxide (WO3) thin films," *Mater. Chem. Phys*., vol. 114, no. 1, pp. 475–478, 2009, doi: 10.1016/j.matchemphys.2008.09.071.

[12] I. M. Ibrahim, "The effect of gold nanoparticles on WO3 thin film," *Iraqi J. Phys*., vol. 16, no. 36, pp. 11–28, 2018, doi: 10.30723/ijp.v16i36.22.

[13] A. R. Siekkinen, J. M. McLellan, J. Chen, and Y. Xia, "Rapid synthesis of small silver nanocubes by mediating polyol reduction with a trace amount of sodium sulfide or sodium hydrosulfide," *Chem. Phys. Lett*., vol. 432, no. 4–6, pp. 491–496, 2006, doi: 10.1016/j.cplett.2006.10.095.

[14] L. M. Liz-Marzán, "Tailoring surface plasmons through the morphology and assembly of metal nanoparticles," *Langmuir*, vol. 22, no. 1, pp. 32–41, 2006, doi: 10.1021/la0513353.

[15] R. Shukla, V. Bansal, M. Chaudhary, A. Basu, R. R. Bhonde, and M. Sastry, "Biocompatibility of gold nanoparticles and their endocytotic fate inside the cellular compartment: a microscopic overview," *Langmuir*, vol. 21, no. 23, pp. 10644–10654, 2005.

[16] K. S. Usha, R. Sivakumar, C. Sanjeeviraja and M. Ichimura, "Physical properties of rf magnetron sputter deposited NiO:WO3 thin film," *Mater. Res. Express*, vol. 2, no. 1, p. 016401, 2015.

[17] B. D. Cullity, *Elements of X-ray Diffraction. Addison-Wesley Publishing*, 1956.

[18] G. A. Al-Dahash, Q. M. Salman, and S. F. Haddawi, "Study the Effect of Copper (Cu) Doping on the Structure Properties of Zinc Oxide (ZnO) Prepared by Using Pulsed Laser Deposition (PLD)," *J. Univ. kerbala*, vol. 15, no. 2, pp. 87–95, 2017.

[19] G. K. Williamson and R. E. Smallman, "III. Dislocation densities in some annealed and cold-worked metals from measurements on the X-ray debye-scherrer spectrum," *Philos. Mag.:A journal of experimental and applied physics*, vol. 1, no. 1, pp. 34–46, 1956.

[20] M. D. R. & K. A. A. G. H.Mohamed , S. N. Mazhir, ―The Influence of Bi content on The Structural and Optical Properties of thin TiO2 (1-x): Bix Films Prepared by pulse laser deposition,‖ *Int. J. Eng. Trends Technol*., vol. 23, 2015.

[21] R. Eason, *Pulsed laser deposition of thin films: applications-led growth of functional materials. John Wiley & Sons*, 2007.

[22] H. Kim and C. M. Gilmore, "Transparent conducting aluminum-doped zinc oxide thin films for organic light-emitting devices," *Appl. Phys. Lett.*, vol. 76, no. 3, pp. 259–261, 2000.

[23] S. Sami, S. S. Chiad, K. Haneen, T. Mubarak, N. F. Habubi, M. K. Mohammed, and A. Khadyair, "Fabrication and study the structure, optical and dispersion parameters of PMMA with InCl3 additive," *J. Glob. Pharma Technol*., vol. 11, no. 4, pp. 369–374, 2019.

[24] M. G. Hutchins, O. Abu-Alkhair, M. M. El-Nahass, and K. Abd El-Hady, "Structural and optical characterisation of thermally evaporated tungsten trioxide (WO3) thin films," *Mater. Chem. Phys*., vol. 98, no. 2–3, pp. 401–405, 2006.

[25] S. J. Mousavi, ―First–Principle Calculation of the Electronic and Optical Properties of Nanolayered ZnO Polymorphs by PBE and mBJ Density Functionals,‖ *J. Optoelectron. Nanostructures*, vol. 2, no. 4, pp. 1–18, 2017.

[26] M. Thakurdesai, N. Kulkarni, B. Chalke, and A. Mahadkar, "Synthesis of CdSe Films by Annealing of Cd/Se Bilayer," *Chalcogenide Lett*., vol. 8, no. 3, pp. 223–229, 2011.

[27] S. Sönmezoğlu, A. Arslan, T. Serin, and N. Serin, "The effects of film thickness on the optical properties of TiO2–SnO2 compound thin films," *Phys. Scr*., vol. 84, no. 6, p. 65602, 2011.

[28] A. Gultekin, "Effect of Au Nanoparticles Doping on The Properties of TiO2 Thin Films", *Materials Science* (Medžiagotyra), vol. 20, no. 1, pp. 1392–1320, 2014.

[29] D. Na, L. Satyanarayana, G.-P. Choi, Y.-J. Shin, and J. S. Park, "Surface morphology and sensing property of NiO-WO3 thin films prepared by thermal evaporation," *Sensors*, vol. 5, no. 12, pp. 519–528, 2005.